Agricultural and Forest Meteorology 264 (2019) 138–148

Contents lists available at ScienceDirect

Agricultural and Forest Meteorology

journal homepage: www.elsevier.com/locate/agrformet

Changes in plant biomass induced by soil moisture variability drive interannual variation in the net ecosystem CO_2 exchange over a reclaimed coastal wetland

Xiaojing Chu[a,b], Guangxuan Han[a,*], Qinghui Xing[a,b], Jianyang Xia[c], Baoyu Sun[a,c], Xinge Li[d], Junbao Yu[a,e], Dejun Li[f], Weimin Song[a]

[a] Key Laboratory of Coastal Environmental Processes and Ecological Remediation, Yantai Institute of Coastal Zone Research, Chinese Academy of Sciences, Yantai, 264003, China
[b] University of Chinese Academy of Sciences, Beijing, 100049, China
[c] School of Ecological and Environmental Sciences, East China Normal University, Shanghai, 200241, China
[d] College of Environment and Planning, Henan University, Kaifeng, 475004, Henan, China
[e] School of Resources and Environmental Engineering, Ludong University, Yantai, 264025, China
[f] Institute of Subtropical Agriculture, Chinese Academy of Sciences, Changsha, 410215, China

ARTICLE INFO

Keywords:
Precipitation
Plant biomass
Net ecosystem CO_2 exchange
Salt stress
Waterlogged stress
Reclaimed coastal wetland

ABSTRACT

Changes in the timing and magnitude of precipitation is a threat to agricultural productivity and farmland carbon stocks. However, the relationship between inter-annual variations in precipitation and net ecosystem CO_2 exchange (NEE) remains to be clarified, particularly when combined with water-salt transport in reclaimed coastal wetland. Here, based on the eddy-covariance technique, we investigated the interannual variation in carbon dioxide exchange and its control mechanism over a reclaimed coastal wetland of the Yellow River Delta from 2010 to 2014. The coastal wetland functioned as a strong sink for atmospheric CO_2, with the annual NEE of -229, -175, -142, -92 and $-80\ g\ C\ m^{-2}$ in the 5 years from 2010 to 2014, respectively. Surprisingly, we find that large annual variation in net ecosystem exchange (NEE) can be predicted accurately using plant biomass. Plant biomass was driven by soil water content (SWC), with about 48%–80% seasonal variation of biomass attributed to SWC. During the early growing stage, high SWC accompanied with low salinity promoted plant biomass and NEE. While high SWC accompanied with increased waterlogged stress inhibited plant biomass and NEE during the middle growing stage. The same results were also observed in a field manipulation experiment over a nearby natural coastal wetland. Our study indicated that extreme climate accompanied with extreme drought and flooding may decrease carbon sequestration capacity of the reclaimed coastal wetland due to the increase in salinity.

1. Introduction

Coastal wetlands play an important role in the global carbon cycle by acting as natural "blue carbon" sinks due to high primary productivity and the low soil organic matter decomposition rate (Bridgham et al., 2006; Crooks et al., 2011; Zhong et al., 2016). However, as the agricultural production bases, large areas of natural coastal wetlands around the world have been reclaimed by human-constructed dykes to satisfy the land demands driven by economic development and population growth in coastal zones (O'Connell, 2003; Vitoarmando et al., 2009; Verhoeven and Setter, 2010 Kirwan and Megonigal, 2013). In China, more than half of salt marshes have been reclaimed for other land uses, which exceeds the area of China's marshes today (Han et al., 2014a, b). The management, such as plough, fertilization and irrigation have not only changed the nutrient cycling (Campbell et al., 2011; Hunt et al., 2013) but also brought great uncertainty to ecosystem C functions and services in the reclaimed coastal wetland.

In addition to artificial factors, natural factors also have a significant impact on ecosystem CO_2 exchange of the reclaimed coastal wetland. Most area of a reclaimed coastal wetland lies beyond the reach of the tides, and its hydrologic regimes is dominated by the interaction of precipitation and a shallow, saline water table in the vertical direction

* Corresponding author at: Key Laboratory of Coastal Zone Environmental Processes and Ecological Remediation, Yantai Institute of Coastal Zone Research, Chinese Academy of Sciences, 264003, Yantai, Shandong, China.
E-mail address: gxhan@yic.ac.cn (G. Han).

https://doi.org/10.1016/j.agrformet.2018.09.013
Received 10 May 2018; Received in revised form 11 September 2018; Accepted 14 September 2018
Available online 18 October 2018
0168-1923/

(Zhang et al., 2011; Han et al., 2015). The hydraulic connection between soil water and groundwater controls the crop growth by directly influencing the water and salt conditions in the soil (Xie and Yang, 2013; Han et al., 2018). Coupled with deficient fresh water (precipitation or irrigation) supply, the water-soluble salts from the groundwater are transported upward to the root zone and soil surface through capillary rise and evaporation (Yao and Yang, 2010). Exposed to limited freshwater inputs, high salt concentrations in soil lead to osmotic and ionspecific stress as well as to imbalances in plant nutrient uptake (Setia et al., 2010). Such changes have a direct negative impact on the activities of plant and soil microbes and ultimately on plant biomass (Lund et al., 2010; Rajan et al., 2013). The existing researches have found that increased salinity combined with decreased soil moisture, and decreased salinity is related increased soil moisture (Chen et al., 2017a, b; Chu et al., 2018). Therefore, lower soil moisture coupled with higher soil salinity is expected to decrease plant biomass in the reclaimed coastal wetland.

On the other hand, as precipitation or irrigation occurs, while inputs of fresh water can leach salts from the plant root zone, soil saturation even episodic flooding is often observed due to the shallow water table (Han et al., 2015). When the reclaimed coastal wetlands are inundated, the effective photosynthetic leaf area may be reduced as some plant leaves are submerged (Schedlbauer et al., 2010), which decreased maximum photosynthetic rate (Chen et al., 2017a, b). Meanwhile, flooding force stomatal closure and transpiration cessation (Banach et al., 2009; Moffett et al., 2010), which affect plant photosynthesis and autotrophic respiration (Schedlbauer et al., 2010). Furthermore, as soil become waterlogged, the saturation of surface soils limits the diffusion of oxygen into soil, which decrease heterotrophic respiration (Heinsch et al., 2004). Subsequently, plant growth is inhibited due to the suppressed photosynthesis and respiration. Therefore, exposed to shallow and salinity groundwater, inputs of freshwater might greatly affect the ecosystem carbon fluxes by affecting the plant biomass (Heinsch et al., 2004; Jimenez et al., 2015)

As a typical coastal wetland, the Yellow River Delta is one of the most active regions of land-ocean interaction among the large river deltas in the world. In addition to its rich biodiversity-supporting capacity, the solid CO_2 sink function of this natural (unreclaimed) coastal wetland has already been confirmed (Han et al., 2013, 2014a, b; Han et al., 2015). However, the Yellow River Delta has been undergoing frequent land reclamations over past decades (Zhang et al., 2011; Huang et al., 2012), and most of its land area was derived from reclaiming vegetated coastal wetlands. The reclaimed farmland is connected to an irrigation system which draws from the Yellow River. Because of the shortage of fresh water, agriculture consumes the largest part of water resources in the Yellow River Delta (Fan et al., 2012), mainly using for irrigation. However, in recent years, the runoff of the Yellow River has decreased dramatically (Cui and Li, 2011; Fu et al., 2004), which brought great impacts on agricultural irrigation. Due to the increasingly strained problem on the source of freshwater supply, the reclaimed coastal wetland is typical rain fed farming areas (Han et al., 2014a, b). The negative effect of the salinity and waterlogged stress on crop productivity thus increased the susceptibility to soil erosion and crop failure.

Global climate models project that alterations in patterns of precipitation regimes represent a rapid and unprecedented change to the fundamental drivers of soil moisture and salinity, which profoundly changed the plant biomass, and eventually altered the carbon budget of ecosystems (Knapp et al., 2008). Here, we use five years (2010–2014) of eddy covariance measurements to explore the annual CO_2 land-atmosphere exchange dynamics and drivers in a reclaimed coastal wetland of the Yellow River Delta, where the hydrologic regimes are mainly dominated by the interaction of precipitation and a shallow, saline water table in the vertical direction. The main objectives were (i) to explore the seasonal and inter-annual variability of NEE, (ii) to identify annual CO_2 sink-source strength, and (iii) to gain new insights into the underlying mechanism of water-salt transport and plant biomass on annual NEE.

2. Materials and methods

2.1. Site description

The research was conducted in a long-term, rainfed, continuous cotton research field, located at a reclaimed coastal wetland in the Yellow River Delta Ecological Research Station of Coastal Wetland (37°45′50″N, 118°59′24″E), which belongs to Yantai Institute of Coastal Zone Research, Chinese Academy of Sciences. Though the site has been reclaimed as a agricultural farmland, it still has the hydrological characteristics of shallow and salinity groundwater in the coastal wetland. During dry seasons, driven by strong evaporation, water-soluble salts from the groundwater are transported upward to the root zone and soil surface through capillary rise. While during rainy season, the episodic flooding is often observed, following heavy rainy events. The area has a warm temperate and continental monsoon climate, with a mean annual air temperature of 12.4 °C. The mean annual precipitation is 401–604 mm, and nearly 88% is concentrated in the growing season. Soil parent materials are alluviums by the Yellow River, and soil texture in the root zone is sandy loam. The farmland, which was reclaimed in April 2008, was used for planting of cotton (*Gossypium hirsutum* L.). Vegetation composition of the ecosystem is simple, and the only vegetation present is cotton. Cotton was planted in middle May at a moderate density (5.3plants m^{-2}) and harvest at the end of Octorber in the Yellow River Delta.

Due to the water shortage, only one-time irrigation was conducted in the spring of 2010. The agricultural was rain-fed and no irrigation has been applied at this site since 2011. After cotton was picked, the cotton plants including roots were harvested and taken away from the fields in order to control pests and diseases or to be burned as domestic fuel. The growing stages of the natural growth cycle were divided from the phenophase. During the early growth stage, defined as the time between sowing time and bud stage, and the biomass increased rapidly during this stage. During the middle growth stage, defined as the period from bud stage to boll stage, the biomass growth is slow during this stage. During the terminal growth stage, representing the time from the boll opening stage to the harvest, the community senesces during this stage.

2.2. Flux and climatic factors measurements

Ecosystem CO_2 fluxes between the reclaimed wetland and the atmosphere were continuously measured using an eddy covariance (EC) system. The open-path EC system was mounted 2.8 m above the soil surface, and fetch length from all directions was more than 300 m. The densities of CO_2 and H_2O were measured by an open-path infrared gas analyzer (IRGA, LI-7500, LI-COR Inc., USA), and the three wind components and the speed of sound were measured with a three-axis sonic anemometer (CSAT-3, Campbell Scientific Inc., USA). Raw data outputs from the IRGA and sonic anemometer were collected at 10 Hz and the averaged flux data were recorded by a data logger (CR1000, Campbell Scientific Inc., USA) averaged at 30 min intervals. The IRGA was calibrated once or twice every year in the laboratory using pure nitrogen gas, CO_2 calibration gas, and a dew point generator (LI-610, Li-COR Inc., USA). As the uniform fetch was at least 300 m in all directions, the majority of fluxes came from the target area.

Meteorological parameters were continuously measured with an array of sensors, including air temperature (HMP45C, Vaisala, Helsinki, Finland), photosynthetic active radiation (PAR) (LI-190SB, Li-Cor Inc., USA), net radiation (CNR4, Kipp & Zonen Netherlands Inc., Bohemia, NY, USA), wind speed and direction (034B, Met One Inc., USA), and precipitation (TE525 tipping bucket gauge, Texas Electronics, Texas, USA). Soil temperature at 5, 10, 30, and 50 cm depths below the surface

(109SS, Campbell Scientific Inc., USA), and soil water content (SWC) at 5, 10, 20, 40, 60, 80, and 100 cm depths below the surface (EnviroSMART SDI-12, Sentek Pty Ltd., Australia) were measured in situ monitoring around the flux tower. All meteorological data were measured every 15 s and then averaged half hourly and stored in a data logger (CR1000, Campbell Scientific Inc., USA).

Biomass of above- and below-ground for the reclaimed coastal wetland was measured by harvesting the vegetation approximately twice a month during the growing season (from May to October) from 2010 to 2014. Harvesting was performed in five replicated sampling plots (0.5 m × 0.5 m) located within a radius of 200 m around the EC system (Han et al., 2014a, b). Live crops were uprooted. Crop biomass of above- and below-ground was oven dried at 80 °C to a constant weight before weighing.

2.3. Flux data treatment

The half-hourly CO_2 flux was calculated using the Edire software (University of Edinburg, Scotland). The 10-Hz raw eddy covariance data were applied to screen out anomalous values, and the filtered data were used to calculate half-hourly CO_2 fluxes. The Webb-Pearman-Leuning (WPL) correction and three-dimensional coordinate rotation (3-D rotation) were used to adjust the half-hourly CO_2 flux data (Webb et al., 1980; Baldocchi et al., 1988). Then, quality tests on stationarity and turbulence development conditions of the half-hourly CO_2 flux data were performed using the software, allocating quality signals to every data point (Mauder and Foken, 2004). In the reclaimed coastal weland, the CO_2 flux storage was neglected because the vegetation canopy height was low (approximately 1 m during the peak growing season) (Anthoni et al., 1999; Baldocchi et al., 2000)

The half-hourly CO_2 flux data outputted by Edire were further filtered according to a series of standards before they were used for later analysis. The excluded data mainly included the following: (1) the half-hour flux data before and after precipitation. (2) The CO_2 flux data whose absolute value (|NEE|) exceeded 60 μ mol CO_2 $m^{-2} s^{-1}$. (3) the CO_2 flux data when the air turbulence was weak, especially when friction velocity (u*) < 0.15 m s^{-1}. The threshold was derived from the scatter plot of u* vs. nighttime CO_2 flux data points according to Schedlbauer et al. (2010), below which the nighttime CO_2 flux data showed a discrete distribution. (4) The CO_2 flux data that were smaller than zero when R_n < 10 W m^{-2}.

We used the following procedure to fill missing and bad data to provide estimates for the balance of NEE. Small gaps (less than 2 h) were filled by linear interpolation. Large gaps (more than 2 h) were filled based on separate empirical models for daytime and nighttime data. When PAR was > 10 μmol m^{-2} s^{-1}, the missing daytime NEE data during the growing season were gap filled using the Michaelis–Menten model (Ruimy et al., 1995; Falge et al., 2001),

$$NEE = -\frac{A_{max}\,\alpha PAR}{A_{max} + \alpha PAR} + R_{eco,\,day} \quad (1)$$

where the coefficient α is the apparent quantum yield (mg CO_2 μmol^{-1} photon), A_{max} is the light-saturated net CO_2 exchange (mg CO_2 m^{-2} s^{-1}), and $R_{eco,day}$ is the daytime ecosystem respiration (mg CO_2 m^{-2} s^{-1}) and PAR is the photosynthetically active radiation (μmol m^{-2} s^{-1}).

When PAR was < 10 μmol m^{-2} s^{-1}, the missing nighttime NEE data were filled with the exponential relationship between R_{eco} and the air temperature at 5 cm (Lloyd and Taylor, 1994):

$$R_{eco,\,night} = a\exp(bT) \quad (2)$$

where $R_{eco,night}$ is the nighttime NEE, T is the air or soil temperature (°C), and a and b are two empirical coefficients.

Daily R_{eco} is the sum of daytime ecosystem respiration ($R_{eco,day}$) and the nighttime ecosystem respiration ($R_{eco,night}$):

$$R_{eco} = R_{eco,day} + R_{eco,night} \quad (3)$$

Daily gross primary productivity (GPP) was calculated as follows:

$$GPP = R_{eco} - NEE \quad (4)$$

The energy balance closure of the study site was assessed by calculating the energy balance ratio (EBR) using the method described by Wilson et al. (2002). The calculated mean EBR for the site from 2010 to 2014 was 0.83, which was presumed an ideal condition for the eddy covariance method (Wilson et al., 2002)

2.4. Precipitation manipulation experiment

The precipitation manipulation experiment was initiated in July of 2014 over an uncultured coastal wetland, 600 m away from the EC tower. The vegetation is relatively homogeneous and strongly dominated by common reed (*Phragmites australis*), with other associated species including *Tamarix chinensis*, *Tripolium vulgare*, *Suaeda salsa* and *Imperata cylindrical*. The experiment was completely randomized block designed, consisting of twenty 3 × 4 m^2 plots, with 4 replicates each consisting of five levels of precipitation [wet (+40%, +60%), drought (-40%, -60%) and ambient (CK)].

The experiment infrastructure used passive removal and active distribution systems to manipulate precipitation. Above the decreased zones, rainout shelters with 24 and 16 of 10-cm-wide corrugated clear polycarbonate slats distributed evenly removed 60% and 40% of incoming precipitation, respectively. During the growing seasons, this water drained into storage tanks and were immediately transferred to the +60% and +40% zones via sprinkler systems, to achieve 60% and 40% increase in each precipitation event, respectively.

We measured NEE with an infrared gas analyzer (IRGA; LI-6400, Li-Cor Inc., Lincoln, Nebraska, USA) attached to a transparent chamber (radius: 0.3 m; height: 0.7 m), which covered all the vegetation within the plastic frame. The experiment was measured under natural (NEE) and shady (R_{eco}) conditions at 2-week intervals (8:00-11:00 h) from April 2018, i.e. after 4 years of consecutive manipulation. GPP was simply the difference between NEE and R_{eco} (Eq. (4)). Data used in this article was from April to June. During the measurement, the chamber was sealed to the frame surface. Two small electric fans were running continuously to promote air mixing within the chamber during the measurement. Increases in air temperatures within the chamber during the measuring time period were less than 0.2°C. CO_2 concentrations were allowed to build up or draw down over time, from which flux rates were determined from the time-course of the concentration to calculate NEE. This static-chamber method has been used and validated in many previous studies (Bubier et al., 2007; Niu et al., 2010). NEE values measured by the canopy chamber were similar to that measured using eddy covariance technique which was set up adjacent to our study site (Han et al., 2015; Chu et al., 2018), illustrating the validity of the canopy chamber method for ecosystem gas exchange measurements. In the experiment, SWC and soil salinity at 10 cm depth approximately were measured every 30 min using sensors of 5TE (Decagon, USA).

2.5. Statistical analysis

Before statistical analysis, data normality was tested using the Kolmogorov-Smirnov test, and square root or natural-log transformation was used as necessary. The relationships between the biophysical variables and NEE were tested using linear and nonlinear regressions. Stepwise multiple linear regressions (using P = 0.05 for entry into the model) based on daily mean data were used to identify which variables explained the variations in NEE and biomass for the entire year and diffferent seasons. Probabilities less than 0.05 were considered significant for all statistical analyses. In the precipitation manipulation experiment, soil salinity, SWC and NEE were calculated as the mean of four replicates at random locations for each treatment. We used the

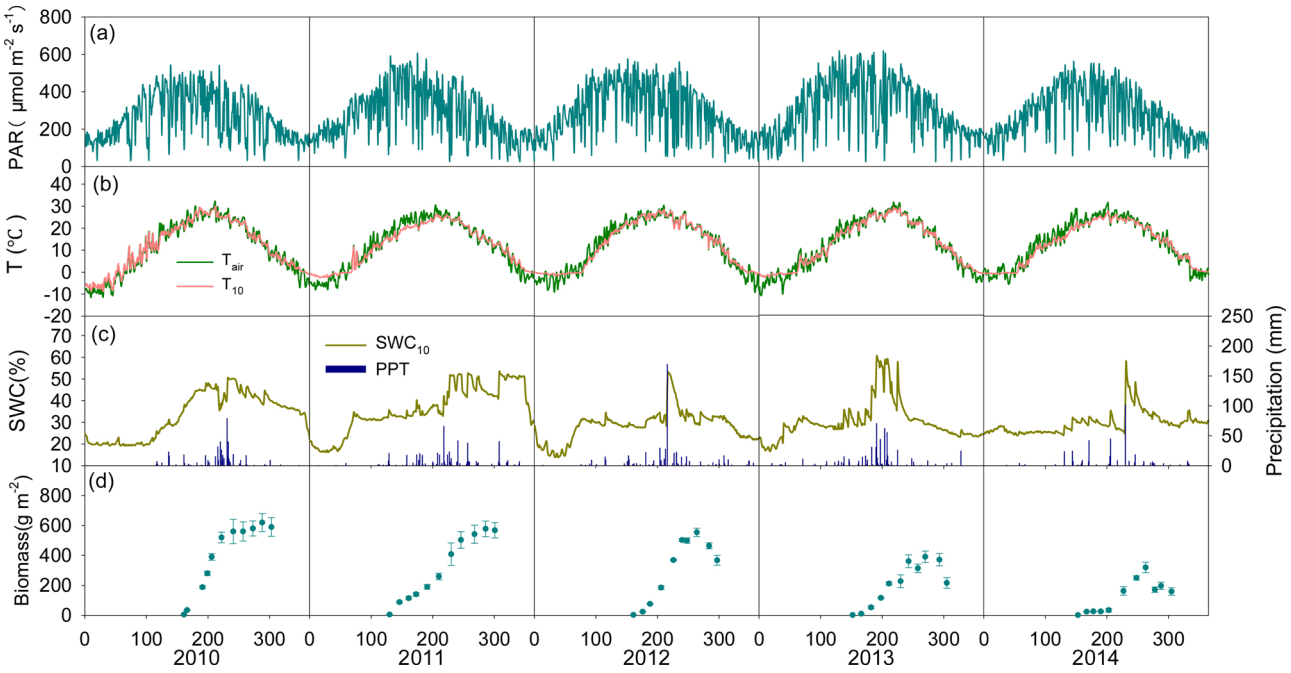

Fig. 1. Seasonal and interannual variations of (a) photosynthetic active radiation (PAR), (b) air temperature (T_{air}) and soil temperature (T_{soil}) at 10 cm depth, (c) daily total precipitation and average volumetric soil water content (SWC) at 10 cm depth, (d) biomass for the period of 2010–2014.

repeated measure analysis of variance (ANOVA) to test the differences in SWC, soil salinity, GPP and NEE. All statistical analyses were performed using SPSS 17.0 (SPSS Inc., Chicago, IL, USA).

3. Results

3.1. Interannual variations in meteorology and plant biomass

The seasonal patterns of PAR, T_{air}, and T_{10} were similar among the five years (Fig. 1a–c). Annual mean PAR ranged from 261 W m^{-2} in 2010 to 304 W m^{-2} in 2013. The average annual temperatures were generally close (within 1.0℃) to the long-term (1961–2009) average of 12.7℃ (Table 1). The variation of the soil temperature at 10 cm was consistent with the air temperature during the five years (Fig. 1b and c).

Annual mean precipitation of the five years was 527 mm, ranging from 401 mm (2014) to 604 mm (2013). In general, the growing season received most (~80%) of the annual precipitation; and winter and early spring were rainless (Fig. 1d, Table 1). At our site, little rain or snow occurred from late autumn to early-spring, so that early-spring SWC_{10} following soil thaw was similar to the values from the preceding autumn. Despite this general regime, over the 5-year period, SWC_{10} was the environmental factor that differed markedly in the study years due to the changes in both the amount and pattern of precipitation (PPT) (Fig. 1d and e). However, both annual and the growing season SWC were not correlated with precipitation ($R^2 = 0.04$, $p = 0.75$; $R^2 = 0.03$, $p = 0.36$). The inter-annual variations of PAR, T_{air}, T_{10}, PPT and SWC_{10} expressed in terms of standard deviation (SD) and coefficient of vatiation (CV, %) were limited to ± 18 μmol m^{-} s^{-1} (6.5%), 0.6℃ (4.8%), 0.4℃ (3.3%), 78 mm (14.8%), and 4.9 (16.2%), respectively (Table 1).

Clear seasonal cycles were observed for biomass, and its seasonal variation patterns differed markedly among years (Fig. 1d). The values of biomass increased rapidly in late June and reached a maximum between September and October, and then followed by a gradual decline as the crop harvest during late October. The seasonal peak value of biomass was highest in 2010 (620 g m^{-2}), while in 2014 the peak value was lowest (197 g m^{-2}).

3.2. Seasonal and interannual variations of ecosystem CO_2 exchange

The courses of ecosystem CO_2 fluxes showed significant seasonal variations, with a net sink of CO_2 during the growing season and a net source of CO_2 for the remainder of the year (Fig. 2, Table 1). It was also subjected to large inter-annual variability, with the site ranging from a strong net CO_2 sink in the 2010 to a weaker net CO_2 sink in 2014

Table 1
Anuual and growing season sums of photosynthetically active radiation (PAR), air temperature (T_{air}), precipitation (PPT), soil t soil water content (SWC) at 10 cm depth, gross primary productivity (GPP), ecosystem respiration (R_{eco}), and net ecosystem CO_2 exchange (NEE).

	PAR (μmol CO_2 m^{-2} s^{-1})		T_{air} (℃)		PPT (mm)		SWC_{10} (%)		GPP (g C m^{-2})		R_{eco} (g C m^{-2})		NEE (g C m^{-2})	
Year	Annual	Growing Season	Annual	Growing Season	Annual	Growing Season	Annual	Growing Season	Annual	Growing Season	Annual	Growing Season	Annual	Growing Season
2010	261	317	12.1	21.4	510	495	34.6	40.5	683	683	458	443	−229	−236
2011	263	336	12.0	21.2	560	466	36.0	39.9	616	616	441	432	−175	−175
2012	291	351	12.1	21.8	561	461	25.4	32.5	605	605	463	449	−142	−150
2013	304	369	12.3	22.0	604	530	25.9	35.4	495	495	402	379	−93	−106
2014	278	339	13.5	21.9	401	370	29.6	31.9	384	384	304	282	−80	−95
Mean	**279**	**342**	**12.4**	**21.7**	**527**	**464**	**30.3**	**36.0**	**557**	**557**	**414**	**397**	**−144**	**−152**
SD	18	19	0.6	0.3	78	60	4.9	4.0	118	118	66	70.0	61	57
CV	6.45	5.56	4.84	1.38	14.80	12.93	16.17	11.11	0.21	0.21	0.16	0.18	0.42	0.37

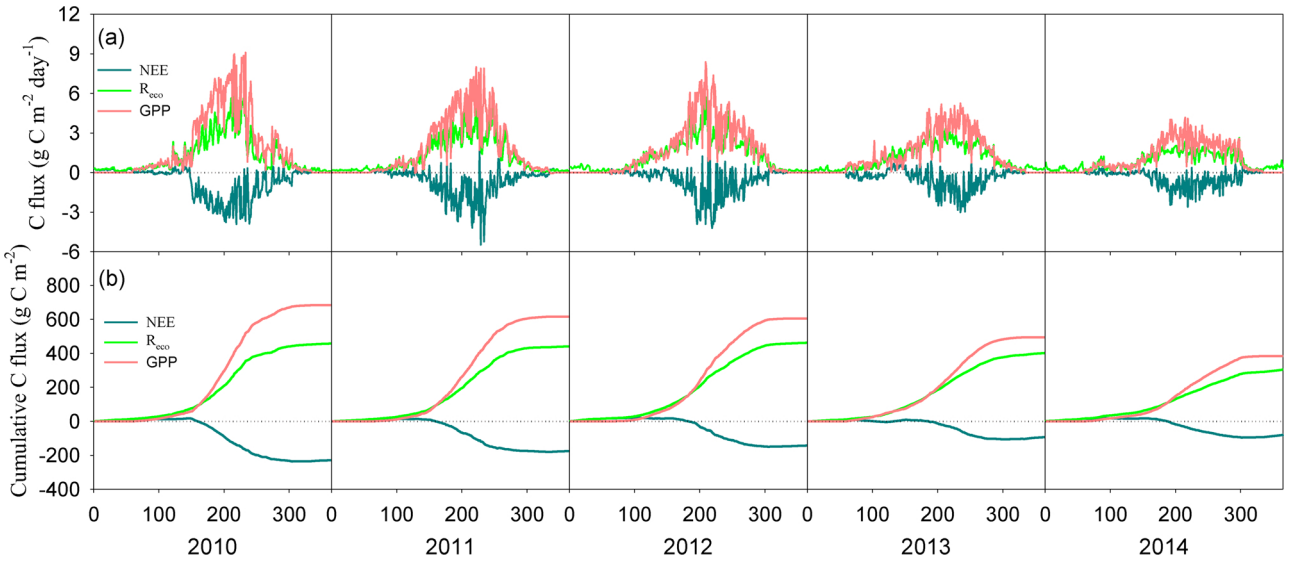

Fig. 2. Seasonal variation in daily average (a) gross primary production (GPP), ecosystem respiration (R_{eco}), net ecosystem CO_2 exchange (NEE), and (b) the cumulative GPP, R_{eco} and NEE over the period of 2010–2014. Each dot represents 1 day. The lines represent the running mean.

(Fig. 2b, Table 1).

Daily NEE varied in the range -3.9 to 0.7, -5.5 to 1.8, -4.2 to 1.8, -3 to 1.1, -2.6 to 0.9 g C m^{-2} day^{-1} in 2010–2014, respectively, where negative values indicate the strength of growing-season C sink (Fig. 2a). During the early growing season, with the seed germination and development of photosynthetic capacity after leaf expansion (Fig. 2a), GPP and R_{eco} increased gradually, the reclaimed coastal wetland became a daily carbon sink as rates of photosynthesis become greater than respiration rates. As time goes on, GPP and R_{eco} increased steadily, with an increasing dominance of GPP over R_{eco}. Large interannual variability was also observed in growing season GPP and R_{eco}: the largest maximal GPP and R_{eco} were observed in 2010 (9.1 g C m^{-2} day^{-1}; 6.9 g C m^{-2} day^{-1}), and the lowest in 2014 (4.2 g C m^{-2} day^{-1}; 2.6 g C m^{-2} day^{-1}). The relationship between NEE and PAR was well described by a rectangular hyperbolic function (Eq. (1)) from 2010 to 2014, and the parameter A_{max} of the model ranged from 0.39 μmol CO_2 m^{-2} s^{-1} in 2014 to 0.65 μmol CO_2 m^{-2} s^{-1} in 2010 (Table 2). $R_{eco,night}$ was positively related to air temperature and could be expressed by the exponential function in all study years ($P < 0.01$, Table 3). The temperature sensitivity coefficient Q_{10} differed markedly in study years with a range of 4.62 in 2010 to 2.52 in 2014 (Table 3).

Overall, the daily average NEE over the growing season in the reclaimed coastal wetland was -1.35, -1.02, -0.92, -0.55 and -0.61 g C m^{-2} d^{-1} for 2010, 2011, 2012, 2013 and 2014, respectively. On the annual scale, the cumulative GPP, R_{eco}, and NEE in all five years showed a high variation (Fig. 2b). The annual cumulative NEE、GPP and R_{eco} for the five years ranged from -92 to −175 g C m^{-2}, 384 to 683 g C m^{-2} and 304 to 463 g C m^{-2}, respectively (Table 1).

Table 2
Coefficients α, A_{max}, and $R_{eco,day}$estimated using Eq. (1) over the period of 2010–2014 in a reclaimed coastal wetland.

	A_{max}(μmol CO_2 m^{-2} s^{-1})	α(μmol μmol $^{-1}$)	$R_{eco,day}$ (μmol CO_2 m^{-2} s^{-1})	n
2010	0.65 ± 0.015	0.001 ± 0.0001	0.13 ± 0.02	3455
2011	0.56 ± 0.0001	0.001 ± 0.0001	0.11 ± 0.014	3607
2012	0.50 ± 0.015	0.001 ± 0.0001	0.12 ± 0.014	3714
2013	0.42 ± 0.01	0.001 ± 0.0001	0.10 ± 0.012	3060
2014	0.39 ± 0.011	0.001 ± 0.0001	0.08 ± 0.009	3489

α, the ecosystem apparent quantum yield; A_{max}, the light-saturated net CO_2 exchange; $R_{eco,day}$, the daytime ecosystem respiration; n, the number of observations. Values of coefficients represent the mean ± SE.

Table 3
Values of coefficients a, b of the equation ($R_{eco,night}$ = aexp(bT)), and Q_{10} of the equation (Q_{10} = exp(10b))over the period of 2010–2014 in a reclaimed coastal wetland.

	a	b	R^2	Q_{10}	n
2010	0.0042	0.153	0.73	4.62	4484
2011	0.0026	0.150	0.75	4.48	4424
2012	0.0096	0.096	0.75	2.61	4425
2013	0.0084	0.093	0.63	2.54	4449
2014	0.0061	0.093	0.36	2.52	4433

a and b, two empirical coefficients; Q_{10}, the temperature sensitivity coefficient; n, the number of observations; R^2, the coefficient of determination.

3.3. Effects of plant biomass on the interannual variability of NEE

Given that many of the environmental variables are auto-correlated and that they co-vary, daily mean data and stepwise multiple linear regressions were applied to derive the major driving variables affecting NEE for the interannual and inter-seasonal timescale. Correlation analysis revealed that biomass was the major driving biological variable of annual CO_2 flux (data not shown).

On interannual timescale, there were a significant negative linear relationship of daily mean NEE values with biomass ($R^2 = 0.93$, $P < 0.01$, Fig. 3a) and a signicicant positive linear relationship of daily mean GPP values with biomass ($R^2 = 0.94$, $P < 0.01$, Fig. 4a). The net CO_2 uptake decreased from year with higher biomass to lower biomass. The significant While on inter-seasonal timescale, daily mean NEE values also exhibited significant ($P < 0.05$) linear correlations with the biomass, coefficient of determination (R^2) with the 95% confidence level, was 0.90 ($P = 0.013$) on the growing season (Fig. 3b) and 0.82 ($P = 0.022$) on the non-growing season (Fig. 3c). In addition, GPP showed positive dependence on biomass during the growing season (Fig. 4b).

On inter-growing seasonal scale, significant negative linear relationships were found between daily mean NEE values and biomass at early and middle growing stages ($P < 0.01$, Fig. 3d and e), whereas the correlation at middle growing stage was stronger ($R^2 = 0.77$). What's more, there were positive linear relationships of GPP with biomass at early and middle growing stages ($P < 0.05$, Fig. 4c and d). No clear response of daily mean NEE or GPP values to biomass was found at the late growing stage as the plant harvest.

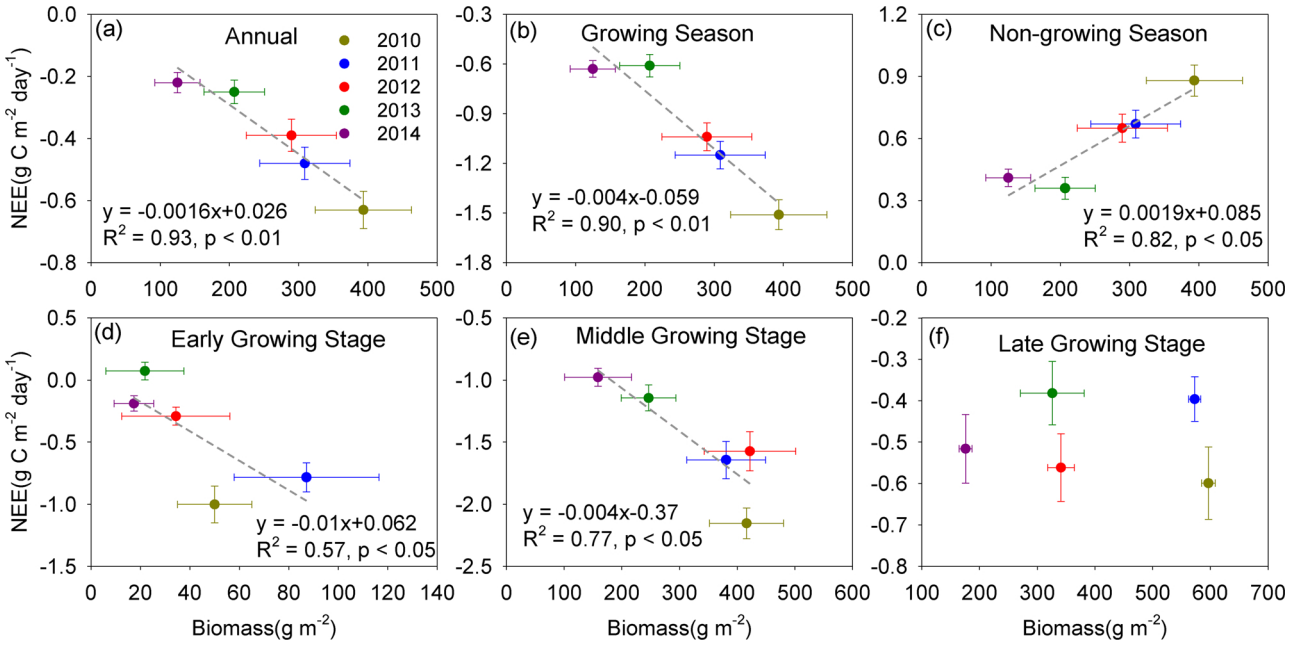

Fig. 3. Relationships between average NEE and biomass during annual (a), growing season (b), non-growing season (c), early growing stage (d), middle growing stage (e), and late growing stage (f) over the period of 2010–2014. Each dot represents 1 year.

3.4. Effects of environmental variables on the interannual variability of plant biomass

The five years differed markedly in the seasonal and annual patterns of biomass (Fig. 2d). To investigate the difference of biomass among years, stepwise multiple linear regressions were applied to derive the major driving variables.

The empirical study on the 5-year monitoring period showed that no significant relationships could be found between annual biomass and major environmental factors (PAR, T and SWC) on the interannual scale ($P > 0.05$). While on the inter-seasonal scale, correlation analysis revealed that biomass was only strongly correlated with the SWC at early

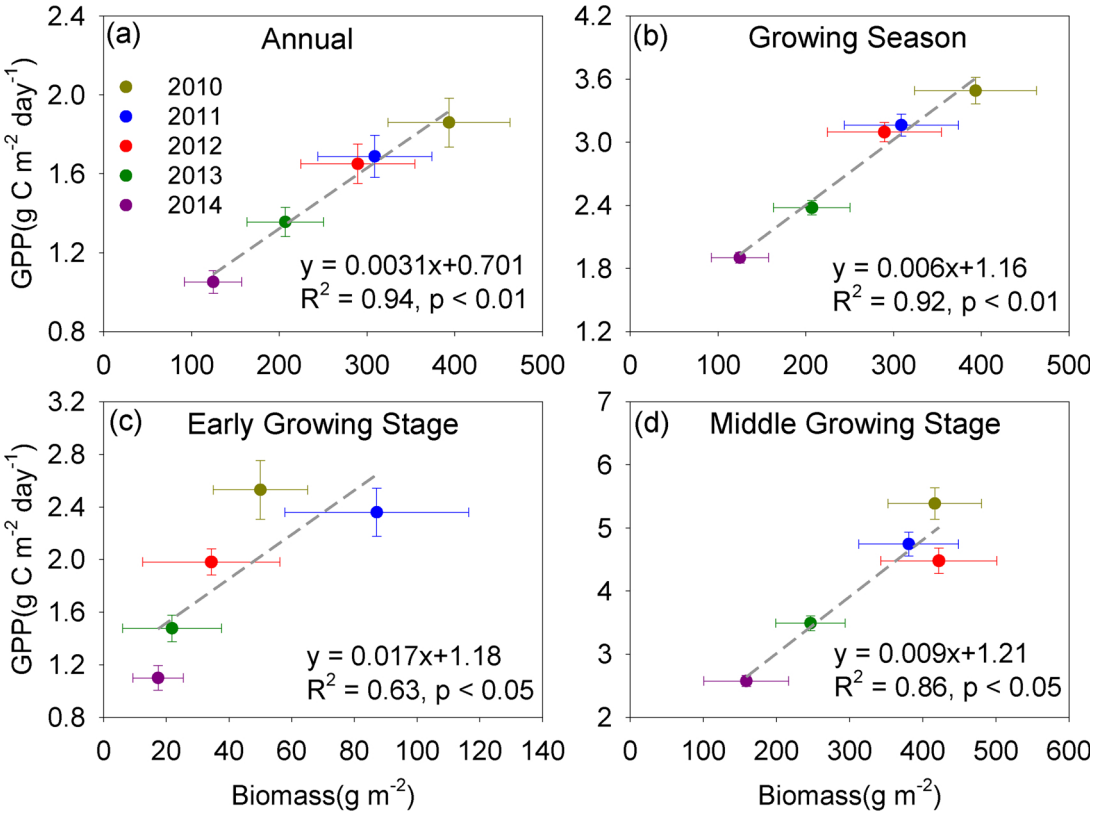

Fig. 4. Relationships between average GPP and biomass during annual (a), growing season (b), early growing stage (c), and middle growing stage (d) over the period of 2010–2014. Each dot represents 1 year.

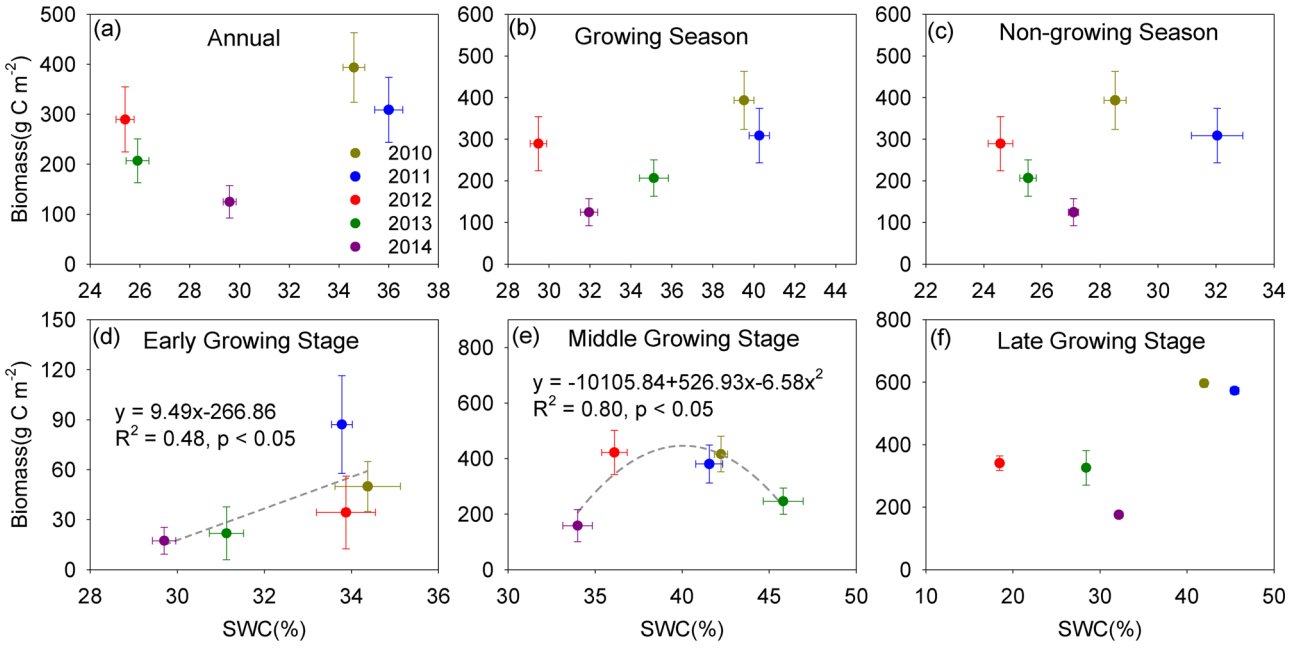

Fig. 5. Relationships between average biomass and SWC during annual (a), growing season (b), non-growing season (c), early growth stage (d), middle growth stage (e), and late growth stage (f) over the period of 2010-2013. Each dot represents 1 year.

and middle growing stages ($P < 0.05$, Fig. 5d and e), indicating that SWC played an important role in the seasonal variation of biomass.

A significantly positive correlation was observed between biomass and SWC, and the R^2 with the 95% confidence level was 48% at early growth stage. However, biomass tended to increase with a rise in SWC and, then, decreased obviously with the increase of SWC as SWC above 40% (Fig. 5e) at middle growth stage. Note that at the late growing stage, no significant correlation was observed, and a sharp decrease of biomass, mainly because of a reduction in photosynthesis during leaf senescence and an increase in soil respiration under relatively high temperature.

3.5. Effect of precipitation changes on soil moisture/salinity and ecosystem CO_2 exchange

On average, precipitation under increased treatments significantly decreased soil salinity, increased SWC, GPP and NEE compared to decreased treatments (Fig. 6, $P < 0.01$) during the early growing stage. SWC significantly decreased with the declines in precipitation and increased with the increases in precipitation (Fig. 6a). There was an overall trend towards decreased salinity with increasing experimental precipitation (Fig. 6b). The soil salinity in the +60% treatment was the lowest, about 28% lower than that in the control. The −60% precipitation treatments had the highest soil salinity, about 53% higher than that in the control (Fig. 6b).

GPP and -NEE both showed a significant increasing pattern with increased precipitation precipitation (Fig. 6c, d). GPP under +60% precipitation treatment was about 63% higher than that in the control, and GPP under -60% precipitation treatment was about 29% lower than that in the control (Fig. 6c). -NEE in the +60% treatment was the highest, about 66% higher than that in the control. The −60% precipitation treatment had the lowest NEE, about 55% higher than that in the control (Fig. 6d).

4. Discussion

4.1. Effects of plant biomass on carbon fluxes

The seasonal and inter-annual variability of NEE reflects the variability of the driving variables at these timescales, as well as changes in the ecosystem's response to these. The significant correlations between biomass and NEE (Fig. 3) illustrates that plant structural characteristics are important for the seasonal and annual ecosystem CO_2 exchange, and the canopy development is an important biological process regulating CO_2 flux in the reclaimed coastal wetland. As the cotton plants still remain in the soil after cotton picking, the significant relationship between NEE and biomass during the non-growing season illustrated some important biotic controls on ecosystem respiration (Janssens et al., 2001; Flanagan and Johnson, 2005). Studies in a reclaimed coastal wetland in the Yangtze Estuary found that the monthly mean NEE was significantly correlated with the monthly mean AGB, suggesting that primary productivity can be well reflected by the aboveground characteristics of higher plant communities (Zhong et al., 2016). This pattern probably occurred because the direct and indirect effects of biomass on plant physiological metabolism process through the activity of photosynthesis and respiration.

Biomass correlated with GPP (Fig. 4), and biomass may affect GPP by changing LAI because leaves in sparse canopies are more likely to be light saturated than those in denser canopies (Springer et al., 2005; Kato et al., 2006; Cheng et al., 2009; Han et al., 2014a, b; Li et al., 2017). As leaf area determines the amount of available photosynthetic material and the amount of light intercepted by the plant, therefore high LAI allows for high light absorption capacity and strong photosynthetic CO_2 uptake on an ecosystem scale (Lund et al., 2010; Wang et al., 2016; Tong et al., 2017). As a result, photosynthesis (GPP) is enhanced (Han et al., 2013; Wang et al., 2015). This interpretation is consistent with observations globally. For example, based on synthesizing data on CO_2 exchange obtained from 12 wetland sites, Lund et al. (2010) found that annual GPP correlated significantly with LAI in those wetland sites. In the Qinghai-Tibetan Plateau shrubland, monthly LAI showed a strong correlation with monthly GPP over 10 years (Li et al., 2016). In an alpine meadow on the Tibetan Plateau, on a monthly scale, 81% of the variation in NEEsat (NEE at the saturated light level) could be explained by the mean NDVI (normalized difference vegetation index) in 4 years (Wang et al., 2016). In an irrigated and rainfed maize field, daytime NEE was closely linked to LAI regardless of the growth stage (Suyker et al., 2004), and similar findings were also found in a rain-fed winter wheat ecosystem of the Loess Plateau (Wang et al.,

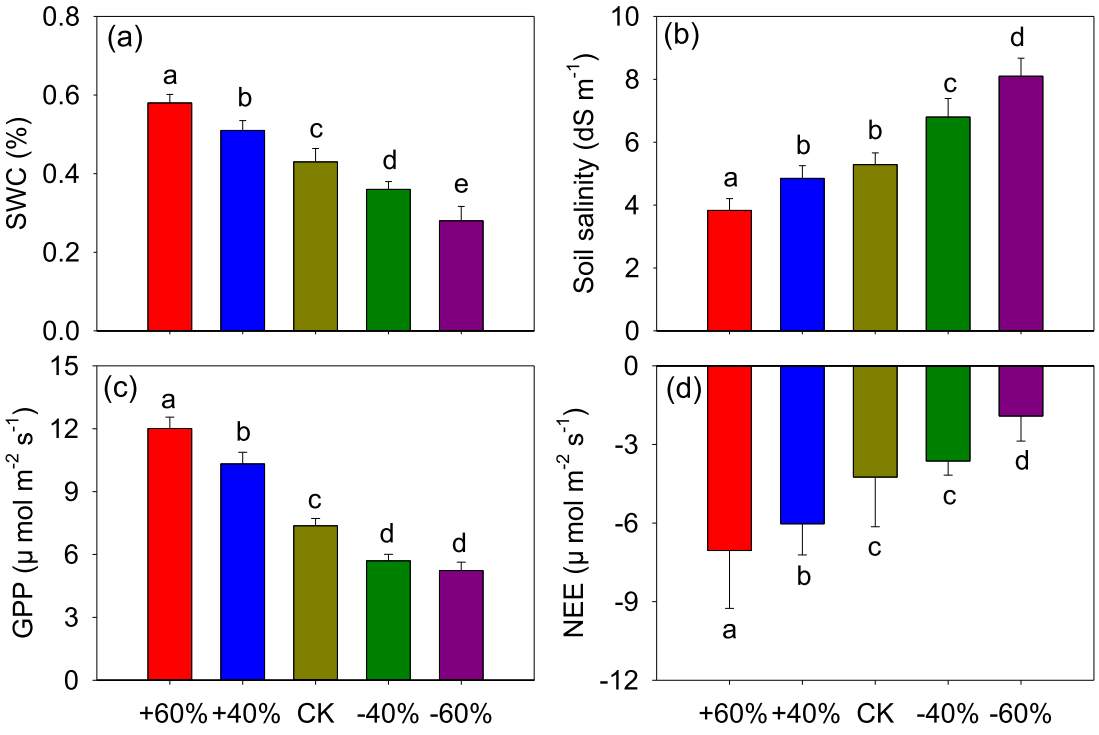

Fig. 6. Effect of changes in precipitation amount on SWC at 10 cm depth (a), soil salinity at 10 cm depth (b), gross primary productivity (c) and net ecosystem CO_2 exchange (d) during the early growing stage in 2018. Different letters (a, b, c, d, e) indicate significant differences among different treatments. Bars represent means ± SE. + 60%: precipitation increased by 60%; + 40%: precipitation increased by 40%; CK: no processing; − 40%: precipitation reduced by 40%; − 60%: precipitation reduced by 60%.

2013).

Studies have found that aboveground respiration contributed significantly to R_{eco}, in addition, biomass is good proxy for accounting for variation in both autotrophic and heterotrophic capacity for respiration (Flanagan and Johnson, 2005; Han et al., 2014a, 2014b; Tong et al., 2017). On the one hand, canopy photosynthesis induced by biomass can modulate aboveground autotrophic respiration by controlling the assimilate supply. The magnitude of autotrophic respiration is influenced by the amount and activity of plants and so reflects changes in plant growth and development, photosynthesis and carbon allocation patterns (Flanagan and Johnson, 2005; Li et al., 2016; Xu et al., 2017). On the other hand, through regulating substrate availability and fresh litter input, the increase in aboveground production implied an increase in total root carbon allocation thus enhanced soil respiration (Yuste et al., 2004; Tong et al., 2017). Soil respiration is the sum of an autotrophic component by roots and the associated rhizosphere and a heterotrophic component by soil microorganisms that decompose the organic materials from both above and below-ground litter (Inouye et al., 1999; Han et al., 2014a, b; Yu et al., 2017). The autotrophic component largely depends on the amount of photosynthates translocated from the aboveground part of the vegetation (Högberg et al., 2001; Yan et al., 2011). The heterotrophic component is dependent on the supply of respiratory (primarily from plant litter and plant root exudates) as well as environmental conditions that control microbial growth and development, and the supply and quality of respiratory substrate provided by biomass, particularly plant roots biomass (Flanagan and Johnson, 2005; Davidson et al., 2006; Matteucci et al., 2015). Studies found that changes in basal rates in soil and root respiration can occur through differences in leaf litter fall (Granier et al., 2008) and photosynthetic activity (Tang et al., 2005) caused by biomass.

4.2. Effects of SWC on plant growth

We observed significantly lower plant productivity in plots with reduced precipitation and increased salinity (Fig. 6). Consistent with our study, Mchugh and Schwartz (2015) showed that adaptaion to water limitation often involves a trade off with plant biomass. SWC may directly or indirectly affect the uptake of CO_2 during photosynthesis (GPP) and the emissions of CO_2 via respiration as well as decomposition (R_{eco}) in several aspects, which subsequently affect biomass in the reclaimed coastal wetland (Fig. 7). As a result, the biomass of the reclaimed coastal wetland is highly dependent on SWC. Higher photosynthetic capacity (per unit of leaf area or photosynthetic pigments or leaf gas exchange) plays an important role in yield improvement of biomass and is significantly affected by the SWC and stages of growing (Chen et al., 2017a, b). Our study showed that SWC dominated biomass by influencing water-salt transport on the annual scale.

During the early growing stage of low SWC, driven by strong evaporation, water-soluble salts from the groundwater are transported upward to the root zone and soil surface through capillary rise (Yao and Yang, 2010; Zhang et al., 2011; Chu et al., 2018). Salt stress may affect biomass through different mechanisms as freshwater becomes limiting. Firstly, seed germination was inhibited in salt stress, starting time of germination delayed, germination rate dropped and embryo axis was growing slow (Pezeshki and Patrick, 1987; Pezeshki et al., 2010a, b). Timing of leaf out affects the length of the growing season, which in turn, can modulate seasonally-integrated photosynthesis (Dong et al., 2011; Jia et al., 2016). Secondly, the soil salinity concentration inhibits leaf emergence and canopy development, resulting in reduced LAI. Salt-induced decreases in canopy LAI also decrease ecosystem autotrophic respiration (both growth and maintenance respiration) (Heinsch et al., 2004). Thirdly, dry air and/or soil conditions may induce plant blade and mesophyll stomatal closure in response to an increase in salinity and a decline in available water (Yang et al., 2016). Reduced LAI combined with stomotal closure can lead to suppressed canopy photosynthetic capacity (Heinsch et al., 2004; Pezeshki et al., 2010a, b; Baldocchi et al., 2017), which decreases the growth rates and biomass of plants. Fields and laboratory studies have indicated that biomass and

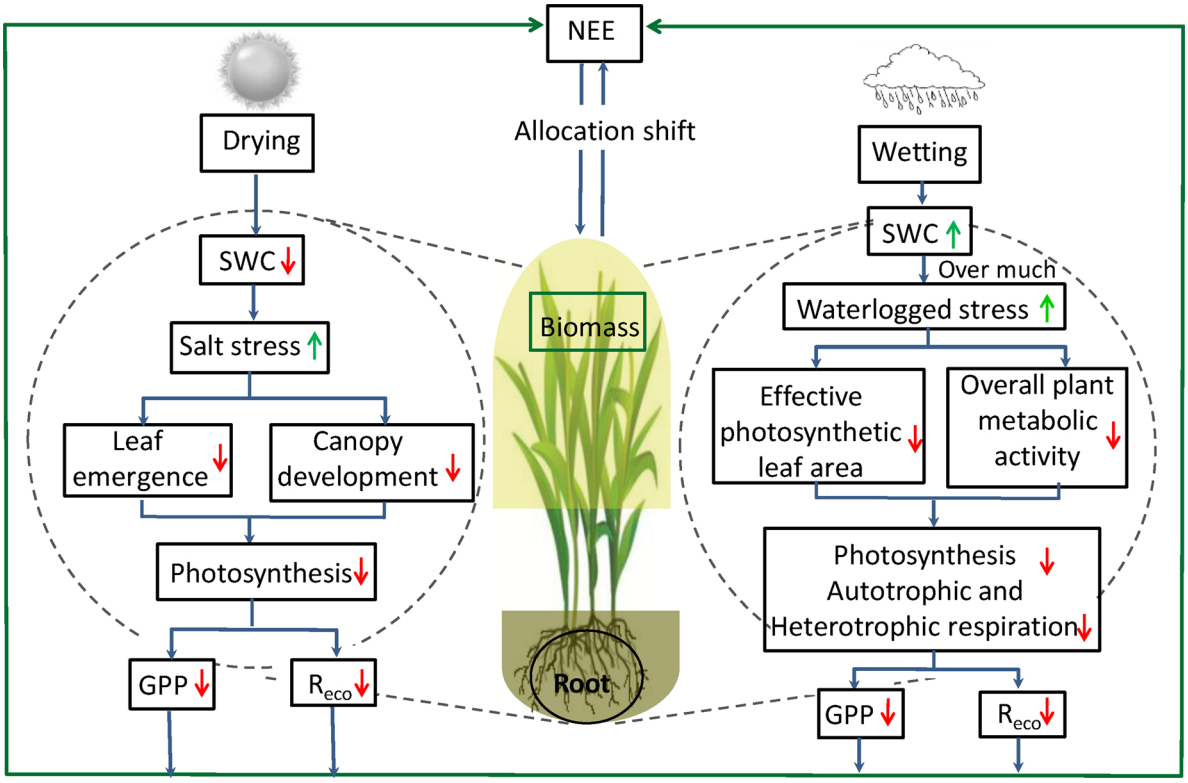

Fig. 7. A schematic diagram illustrating the effect of precipitation-induced changes in plant biomass on the ecosystem CO_2 exchange in a reclaimed coastal wetland. Exposed to limited freshwater inputs, increased soil salinity have a direct negative impact on the activities of plant and soil microbes due to the salt water. After precipitation events, moderate precipitation promote the plant growth. While under humid soil conditions, episodic flooding is often observed due to the shallow water table, which decreased maximum photosynthetic rate and ecosystem respiration. Therefore precipitation-induced changes in plant biomass drive interannual variability of NEE by controlling water-sal transport in soil.

growth rates of many freshwater plants decline as salinities increase (Neubauer, 2013; Johns et al., 2014; Liu and Mou, 2016). The inflow of freshwater after precipitation tends to dilute the salinity and increase SWC in the reclaimed wetland, which may accelerate net photosynthesis rate and promote plant growth, and consequently increase biomass (Fig. 5d). Similar to results reported by Heinsch et al. (2004) who found that gross ecosystem production declined when freshwater availability is low and salinity is high of the Nueces River Delta.

During the middle growing stage, it showed a quadratic trend (80%) between biomass and SWC. Bin-averaged responses of biomass to different SWC classes indicate that biomass increases with increasing SWC up to a threshold of about 40%, above which a shift in biomass towards lower values occurred (Fig. 5e). Our previous study had found that net photosynthetic rate of increased precipitation treatment was significantly suppressed compared to decreased precipitation treatment at the middle growing stage (Chu et al., 2018). As the reclaimed wetland completely entered a monsoon during this period, excess precipitation often caused episodic flooding when SWC became saturated (Han et al., 2015). On the one hand, light conditions mostly determine the dynamics of photosynthesis, a monsoon can depress incoming solar radiation due to increased cloudiness and increase net radiation due to decreased longwave radiation cooling and decreased albedo (Hyojung et al., 2014), as a result, net photosynthetic rate was inhibited. On the other hand, waterlogged stress induced by high precipitation could suppress net photosynthetic rate due to the reduced above-water leaf area of plants (Heinsch et al., 2004), as a result, the net CO_2 uptake was inhibited. In addition, standing water and water in pores restrict the gas exchange between sediments and the atmosphere (Jimenez et al., 2015), and soil hypoxia or anoxia can decrease overall plant metabolic activity and force stomatal closure (Moffett et al., 2010; Schedlbauer et al., 2010). What's worse, as root system is sensitive to drops in oxygen level in soil, prolonged waterlogging can even cause plant to drown because of hypoxia.

4.3. Limitation and prospective

Soil moisture-induced changes in plant biomass drive interannual variability of NEE in a reclaimed coastal wetland. Due to the unique hydrology of salty and shallow underground water in this area, the variation of soil water and salinity makes the coupled transport process very complicated. For lack of instrument of salinity, the concentration of salt as an important abiological process regulating CO_2 flux was not monitored in our study. Though a precipitation manipulation experiment in an unreclaimed coastal wetland has confirmed that lower soil moisture coupled with higher soil salinity, the ecosystems were different. These limited data will increase the uncertainty about the effect of water-salt movement on plant biomass and NEE. Hence, further study and a wider range of salinity, wetland hydrology and other environmental factors are needed to confirm the influence mechanism of water-salt movement on the reclaimed coastal wetlands.

On a global scale, changes in atmospheric circulation drive larger increases in more extreme precipitation events compared with less extreme ones, besides, atmospheric stability increases with warming, weakening circulation and reducing the intensity of precipitation events (Allen and Ingram, 2002; Pendergrass, 2018). On a regional scale, our previous study reveals that the amount and frequency of annual precipitation at this site has decreased by 241.8 mm and 6.9 days over the 55-year interval (1961–2015), respectively. What's more, average annual air temperature at this site has increased by 1.7°C over the past 55 years (Han et al., 2018). Furthermore, the yearly water discharge at the main gauging stations along the Yellow River, all showed significant decreasing trends ($p < 0.01$) over the past six

decades (1951–2010) (Wang et al., 2016), which brought great impacts on agricultural irrigation. Due to the increasingly strained problem on the source of freshwater supply, the reclaimed coastal wetland is typical rain fed farming areas (Han et al., 2014a, b). Considering that extreme climate and runoff of the Yellow River are becoming increasingly variable in future (Wang et al., 2016; Pendergrass, 2018), we speculate that the crop yields would be reduced due to the decreased soil moisture and increased soil salinization, and finally the annual ecosystem CO_2 exchange of the coastal farmland may be suppressed (Yao and Yang, 2010; Xie and Yang, 2013; Rajan et al., 2013).

4.4. Conclusion

Our study indicates that soil moisture-induced changes in plant biomass drive interannual variability of NEE by controlling water-salt transport. During the early growing stage, precipitation or irrigation accompanied with high SWC and low salinity promoted plant biomass and NEE. While precipitation or irrigation accompanied with increased waterlogged stress inhibited plant biomass and NEE during the middle growing stage. Our new insight is particularly valuable under the background of global warming and reduced runoff in the Yellow River, which will help improve the formulation and interpretation of models that are sensitive to differences in the seasonal effects of soil moisture on the CO_2 response.

Acknowledgements

This work was founded by the National Nature Science Foundation of China (41671089), the Science and Technology Service Network Initiative (KFJ-STS-ZDTP-023) and Key deployment project of Chinese Academy of Sciences (KFZD-SW-112). We also thank Liqiong Yang, Min Zhu, Bo Guan, Baohua Xie and two anonymous reviewers of their expert advice and fruitful comments.

References

Allen, M.R., Ingram, W.J., 2002. Constraints on future changes in climate and the hydrologic cycle. Nature 419, 224–232.
Anthoni, P.M., Law, B.E., Unsworth, M.H., 1999. Carbon and water vapor exchange of an open-canopied ponderosa pine ecosystem. Agric. For. Meteorol. 95, 151–168.
Baldocchi, D.D., Hincks, B.B., Meyers, T.P., 1988. Measuring biosphere-atmosphere exchanges of biologically related gases with micrometeorological methods. Ecology 69, 1331–1340.
Baldocchi, D., Finnigan, J., Wilson, K., Paw, U.K.T., Falge, E., 2000. On measuring net ecosystem carbon exchange over tall vegetation on complex terrain. Bound-Lay Meteorol. 96, 257–291.
Baldocchi, D., Chu, H., Reichstein, M., 2017. Inter-annual variability of net and gross ecosystem carbon fluxes: a review. Agric. For. Meteorol. 249, 520–533.
Banach, K., Banach, A.M., Lamers, L.P.M., de Kroon, H., Bennicelli, R.P., Smits, A.J.M., Visser, E.J.W., 2009. Differences in flooding tolerance between species from two wetland habitats with contrasting hydrology: implications for vegetation development in future floodwater retention areas. Ann. Bot. 103, 341–351.
Bridgham, S.D., Megonigal, J.P., Keller, J.K., Bliss, N.B., Trettin, C., 2006. The carbon balance of North American Wetlands. Wetlands 26, 889–916.
Bubier, J.L., Moore, T.R., Bledzki, L.A., 2007. Effects of nutrient addition on vegetation and carbon cycling in an ombrotrophic bog. Glob. Change Biol. 13, 1168–1186.
Campbell, C.A., Lafond, G.P., VandenBygaart, A.J., Zentner, R.P., Lemke, R., May, W.E., Holzapfel, C.B., 2011. Effect of crop rotation, fertilizer and tillage management on spring wheat grain yield and N and P content in a thin Black Chernozem: A long-term study. Revue Canadienne De Phytotechnie 91, 467–483.
Chen, L., Sun, B.Y., Han, G.X., Liu, Z.T., He, W.J., Wang, A.D., Wu, L.X., 2017a. Effects of changes in precipitation amount on soil respiration and photosyntheticc characteristics of Phragmites autralis in a coastal wetland in the Yellow River Delta, China. Chin. J. Appl. Ecol. 28, 2794–2804.
Chen, Z.K., Niu, Y.P., Ma, H., Hafeez, A., Luo, H.H., Zhang, W.F., 2017b. Photosynthesis and biomass allocation of cotton as affected by deep-layer water and fertilizer application depth. Photosynthetica 55, 638–647.
Cheng, X., Luo, Y., Bo, S., Paulsj, V., Hui, D., Daniel, O., Johna, A., Dalew, J., Rdavid, E., 2009. Responses of net ecosystem CO_2 exchange to nitrogen fertilization in experimentally manipulated grassland ecosystems. Agric. For. Meteorol. 149, 1956–1963.
Chu, X., Han, G., Xing, Q., Xia, J., Sun, B., Yu, J., Li, D., 2018. Dual effect of precipitation redistribution on net ecosystem CO_2 exchange of a coastal wetland in the Yellow River Delta. Agric. For. Meteorol. 249, 286–296.
Crooks, S., Herr, D., Tamelander, J., Laffoley, D., Vandever, J., 2011. Mitigating Climate Change through Restoration and Management of Coastal Wetlands and Near-shore Marine Ecosystems: Challenges and Opportunities.
Cui, B., Li, X., 2011. Coastline change of the Yellow River estuary and its response to the sediment and runoff (1976–2005). Geomorphology 127, 32–40.
Davidson, E.A., Janssens, I.A., Luo, Y., 2006. On the variability of respiration in terrestrial ecosystems: moving beyond Q_{10}. Glob. Change Biol. 12, 154–164.
Dong, G., Guo, J., Chen, J., Sun, G., Gao, S., Hu, L., Wang, Y., 2011. Effects of spring drought on carbon sequestration, evapotranspiration and water use efficiency in the songnen meadow steppe in northeast China. Ecohydrology 4, 211–224.
Falge, E., Baldocchi, D., Olson, R., Anthoni, P., Aubinet, M., Bernhofer, C., Burba, G., Ceulemans, R., Clement, R., Han, D., 2001. Gap filling strategies for defensible annual sums of net ecosystem exchange. Agric. For. Meteorol. 107, 43–69.
Fan, X., Pedroli, B., Liu, G., Liu, Q., Liu, H., Shu, L., 2012. Soil salinity development in the Yellow River Delta in relation to groundwater dynamics. Land Degrad. Dev. 23, 175–189.
Flanagan, L.B., Johnson, B.G., 2005. Interacting effects of temperature, soil moisture and plant biomass production on ecosystem respiration in a northern temperate grassland. Agric. For. Meteorol. 130, 237–253.
Fu, G., Chen, S., Liu, C., Shepard, D., 2004. Hydro-Climatic Trends of the Yellow River Basin for the Last 50 Years. Clim. Change 65, 149–178.
Granier, A., Bréda, N., Longdoz, B., Gross, P., Ngao, J., 2008. Ten years of fluxes and stand growth in a young beech forest at Hesse, North-eastern France. Ann. For. Sci. 65 704-704.
Han, G., Yang, L., Yu, J., Wang, G., Mao, P., Gao, Y., 2013. Environmental Controls on Net Ecosystem CO_2 Exchange Over a Reed (*Phragmites australis*) Wetland in the Yellow River Delta, China. Estuar. Coast. 36, 401–413.
Han, G., Luo, Y., Li, D., Xia, J., Xing, Q., Yu, J., 2014a. Ecosystem photosynthesis regulates soil respiration on a diurnal scale with a short-term time lag in a coastal wetland. Soil Biol. Biochem. 68, 85–94.
Han, G., Xing, Q., Yu, J., Luo, Y., Li, D., Yang, L., Wang, G., Mao, P., Xie, B., Mikle, N., 2014b. Agricultural reclamation effects on ecosystem CO_2 exchange of a coastal wetland in the Yellow River Delta. Agr. Ecosyst. Environ. 196, 187–198.
Han, G., Chu, X., Xing, Q., Li, D., Yu, J., Luo, Y., Wang, G., Mao, P., Rafique, R., 2015. Effects of episodic flooding on the net ecosystem CO_2 exchange of a supratidal wetland in the Yellow River Delta. J. Geophys. Res.-Biog. 120, 1506–1520.
Han, G., Sun, B., Chu, X., Xing, Q., Song, W., Xia, J., 2018. Precipitation events reduce soil respiration in a coastal wetland based on four-year continuous field measurements. Agric. For. Meteorol. s256–257, 292–303.
Heinsch, F.A., Heilman, J.L., Mcinnes, K.J., Cobos, D.R., Zuberer, D.A., Roelke, D.L., 2004. Carbon dioxide exchange in a high marsh on the Texas Gulf Coast: effects of freshwater availability. Agric. For. Meteorol. 125, 159–172.
Högberg, P., Nordgren, A., Buchmann, N., Taylor, A.F., Ekblad, A., Högberg, M.N., Nyberg, G., Ottossonlöfvenius, M., Read, D.J., 2001. Large-scale forest girdling shows that current photosynthesis drives soil respiration. Nature 411, 789–792.
Huang, L., Bai, J., Chen, B., Zhang, K., Huang, C., Liu, P., 2012. Two-decade wetland cultivation and its effects on soil properties in salt marshes in the Yellow River Delta, China. Ecol. Inform. 10, 49–55.
Hunt, J.R., Browne, C., Mcbeath, T.M., Verburg, K., Craig, S., Whitbread, A.M., 2013. Summer fallow weed control and residue management impacts on winter crop yield though soil water and N accumulation in a winter-dominant, low rainfall region of southern Australia. Crop Pasture Sci. 64, 922–934.
Hyojung, K., Elise, P., Brente, E., Meagan, C., Kusum, N., 2014. Spring drought regulates summer net ecosystem CO_2 exchange in a sagebrush-steppe ecosystem. Agric. For. Meteorol. 148, 381–391.
Inouye, S., Nakazawa, A., Nakazawa, T., 1999. Soil CO_2 efflux in a beech forest: the contribution of root respiration. Ann. For. Sci. 56, 289–295.
Janssens, I.A., Lankreijer, H., Matteucci, G., Kowalski, A.S., Buchmann, N., Epron, D., Pilegaard, K., Kutsch, W., Longdoz, B., Grunwald, T., Montagnani, L., Dore, S., Rebmann, C., Moors, E.J., Grelle, A., Rannik, U., Morgenstern, K., Clement, R., Oltchev, S., Gudmundsson, J., Minerbi, S., Berbigier, P., Ibrom, A., Moncrieff, J., Aubinet, M., Bernhofer, C., Jensen, N.O., Vesala, T., Granier, A., Schulze, E.-D., Lindroth, A., Dolman, A.J., Jarvis, P.G., Ceulmans, R., Valentini, R., 2001. Productivity overshadows temperature in determining soil and ecosystem respiration across European forests. Glob. Change Biol. 7, 269–278.
Jia, X., Zha, T., Gong, J., Wang, B., Zhang, Y., Wu, B., Qin, S., Peltola, H., 2016. Carbon and water exchange over a temperate semi-arid shrubland during three years of contrasting precipitation and soil moisture patterns. Agric. For. Meteorol. s 228–229, 120–129.
Jimenez, K.L., Starr, G., Staudhammer, C.L., Schedlbauer, J.L., Loescher, H.W., Malone, S.L., Oberbauer, S.F., 2015. Carbon dioxide exchange rates from short- and long--hydroperiod Everglades freshwater marsh. J. Geophys. Res.-Biog. 117 12751-12751.
Johns, C., Ramsey, M., Bell, D., Vaughton, G., 2014. Does increased salinity reduce functional depth tolerance of four non-halophytic wetland macrophyte species? Aquat. Bot. 116, 13–18.
Kato, T., Tang, Y., Gu, S., Hirota, M., Du, M., Li, Y., Zhao, X., 2006. Temperature and biomass influences on interannual changes in CO_2 exchange in an alpine meadow on the Qinghai-Tibetan Plateau. Glob. Change Biol. 12, 1285–1298.
Kirwan, M.L., Megonigal, J.P., 2013. Tidal wetland stability in the face of human impacts and sea-level rise. Nature 504, 53–60.
Knapp, A.K., Beier, C., Briske, D.D., Classen, A.T., Luo, Y., Reichstein, M., Smith, M.D., Smith, S.D., Bell, J.E., Fay, P.A., 2008. Consequences of more extreme precipitation regimes for terrestrial ecosystems. Bioscience 58, 811–821.
Li, H., Zhang, F., Li, Y., Wang, J., Zhang, L., Zhao, L., Cao, G., Zhao, X., Du, M., 2016. Seasonal and inter-annual variations in CO_2 fluxes over 10 years in an alpine shrubland on the Qinghai-Tibetan Plateau, China. Agric. For. Meteorol. 228-229, 95–103.
Li, L., Wang, Y.P., Beringer, J., Shi, H., Cleverly, J., Cheng, L., Eamus, D., Huete, A.,

Hutley, L., Lu, X., 2017. Responses of LAI to rainfall explain contrasting sensitivities to carbon uptake between forest and non-forest ecosystems in Australia. Sci. Rep. 7, 11720.
Liu, Q., Mou, X., 2016. Interactions Between Surface Water and Groundwater: Key Processes in Ecological Restoration of Degraded Coastal Wetlands Caused by Reclamation. Wetlands 36, 95–102.
Lund, M., Lafleur, P.M., Roulet, N.T., Lindroth, A., Christensen, T.R., Aurela, M., Chojnicki, B.H., Flanagan, L.B., Humphreys, E.R., Laurila, T., 2010. Variability in exchange of CO_2 across 12 northern peatland and tundra sites. Glob. Change Biol. 16, 2436–2448.
Matteucci, M., Gruening, C., Ballarin, I.G., Seufert, G., Cescatti, A., 2015. Components, drivers and temporal dynamics of ecosystem respiration in a Mediterranean pine forest. Soil Biol. Biochem. 88, 224–235.
Mauder, M., Foken, T., 2004. Documentation and instruction manual of the eddy covariance software package TK2. P. R. Soc. Med. 43, 181–186.
Mchugh, T.A., Schwartz, E., 2015. Changes in plant community composition and reduced precipitation have limited effects on the structure of soil bacterial and fungal communities present in a semiarid grassland. Plant Soil 388, 175–186.
Moffett, K.B., Wolf, A., Berry, J.A., Gorelick, S.M., 2010. Salt marsh-atmosphere exchange of energy, water vapor, and carbon dioxide: effects of tidal flooding and biophysical controls. Water Resour. Res. 46, 5613–5618.
Neubauer, S.C., 2013. Ecosystem responses of a tidal freshwater marsh experiencing saltwater intrusion and altered hydrology. Estuar. Coast. 36, 491–507.
Niu, S., Wu, M., Han, Y., Xia, J., Zhang, Z., Yang, H., Wan, S., 2010. Nitrogen effects on net ecosystem carbon exchange in a temperate steppe. Glob. Change Biol. 16, 144–155.
O'Connell, M.J., 2003. Detecting, measuring and reversing changes to wetlands. Wetl. Ecol. Manag. 11, 397–401.
Pendergrass, A.G., 2018. What precipitation is extreme? Science 360, 1072–1073.
Pezeshki, S.R., Patrick, W.H., 1987. Effects of flooding and salinity on photosynthesis of Sagittaria lancifolia. Mar. Ecol. Prog. Ser. 41, 87–91.
Pezeshki, S.R., Laune, R.D., Patrick, W.H., 2010a. Response of freshwater marsh species, Panicum hemitomen Schultz, to increased salinity. Freshw. Rev. 17, 195–200.
Pezeshki, S.R., Laune, R.D.D., Jr, W.H.P., 2010b. Response of the freshwater marsh species, Panicum hemitomon Schult., to increased salinity. Freshw. Rev. 17, 195–200.
Rajan, N., Maas, S.J., Song, C., 2013. Extreme drought effects on carbon dynamics of a semiarid pasture. Agron. J. 105, 1749–1760.
Ruimy, A., Jarvis, P.G., Baldocchi, D.D., Saugier, B., 1995. CO_2 fluxes over plant canopies and solar radiation: a review. Adv. Ecol. Res. 26, 1–68.
Schedlbauer, J.L., Oberbauer, S.F., Starr, G., Jimenez, K.L., 2010. Seasonal differences in the CO_2 exchange of a short-hydroperiod Florida everglades marsh. Agric. For. Meteorol. 150, 994–1006.
Setia, R., Marschner, P., Baldock, J., Chittleborough, D., 2010. Is CO_2 evolution in saline soils affected by an osmotic and calcium carbonate. Biol. Fert. Soils 46, 781–792.
Springer, C.J., Delucia, E.H., Thomas, R.B., 2005. Relationships between net photosynthesis and foliar nitrogen concentrations in a loblolly pine forest ecosystem grown in elevated atmospheric carbon dioxide. Tree Physiol. 25, 385.
Suyker, A.E., Verma, S.B., Burba, G.G., Arkebauer, T.J., Walters, D.T., Hubbard, K.G., 2004. Growing season carbon dioxide exchange in irrigated and rainfed maize. Agric. For. Meteorol. 124, 1–13.
Tang, J., Baldocchi, D.D., Xu, L., 2005. Tree photosynthesis modulates soil respiration on a diurnal time scale. Glob. Change Biol. 11, 1298–1304.
Tong, X., Li, J., Nolan, R.H., Yu, Q., 2017. Biophysical controls of soil respiration in a wheat-maize rotation system in the North China Plain. Agric. For. Meteorol. 246, 231–240.
Verhoeven, J.T., Setter, T.L., 2010. Agricultural use of wetlands: opportunities and limitations. Ann. Bot. 105, 155.
Vitoarmando, L., Mariadolores, H., Luigi, B., Antonio, D., Eristanna, P., Michele, P., 2009. Soil chemical and biochemical properties of a salt-marsh alluvial Spanish area after long-term reclamation. Biol. Fert. Soils 45, 691–700.
Wang, W., Liao, Y., Wen, X., Guo, Q., 2013. Dynamics of CO_2 fluxes and environmental responses in the rain-fed winter wheat ecosystem of the Loess Plateau, China. Sci.Total Environ. 461–462, 10–18.
Wang, D., Wu, G.L., Liu, Y., Yang, Z., Hao, H.M., 2015. Effects of grazing exclusion on CO_2 fluxes in a steppe grassland on the Loess Plateau (China). Ecol. Eng. 83, 169–175.
Wang, L., Liu, H., Sun, J., Shao, Y., 2016. Biophysical effects on the interannual variation in carbon dioxide exchange of an alpine meadow on the Tibetan Plateau. Atmos. Chem. Phys. 17, 1–28.
Webb, E.K., Pearman, G.I., Leuning, R., 1980. Correction of flux measurements for density effects due to heat and water vapour transfer. Q. J. R. Meteorol. Soc. 106, 85–100.
Wilson, K., Goldstein, A., Falge, E., Aubinet, M., Baldocchi, D., Berbigier, P., Bernhofer, C., Ceulemans, R., Dolman, H., Field, C., Grelle, A., Ibrom, A., Law, B., Kowalski, A., Meyers, T., Moncrieff, J., Monson, R., Oechel, W., Tenhunen, J., Valentini, R., Verma, S., 2002. Energy balance closure at fluxnet sites. Agric. For. Meteorol. 113 (1), 223–243.
Xie, W.P., Yang, J.S., 2013. Assessment of soil water content in field with antecedent precipitation index and groundwater depth in the Yangtze River Estuary. J. Integr. Agric. 12, 711–722.
Xu, M., Wang, H., Wen, X., Zhang, T., Di, Y., Wang, Y., Wang, J., Cheng, C., Zhang, W., 2017. The full annual carbon balance of a subtropical coniferous plantation is highly sensitive to autumn precipitation. Sci. Rep. 7, 10025.
Yan, L., Chen, S., Huang, J., Lin, G., 2011. Water regulated effects of photosynthetic substrate supply on soil respiration in a semiarid steppe. Glob. Change Biol. 17, 1990–2001.
Yang, Y., Guan, H., Okke, B., Mcvicar, T.R., Long, D., Shilong, P., Liang, W., Liu, B., Jin, Z., Simmons, C.T., 2016. Contrasting responses of water use efficiency to drought across global terrestrial ecosystems. Sci. Rep. 6, 23284.
Yao, R.J., Yang, J.S., 2010. Quantitative evaluation of soil salinity and its spatial distribution using electromagnetic induction method. Agric. Water Manage. 97, 1961–1970.
Yu, S., Chen, Y., Zhao, J., Fu, S., Li, Z., Xia, H., Zhou, L., 2017. Temperature sensitivity of total soil respiration and its heterotrophic and autotrophic components in six vegetation types of subtropical China. Sci. Total Environ. 607–608, 160–167.
Yuste, J.C., Janssens, I.A., Carrara, A.R., 2004. Annual Q10 of soil respiration reflects plant phenological patterns as well as temperature sensitivity. Glob. Change Biol. 10, 161–169.
Zhang, T.T., Zeng, S.L., Gao, Y., Ouyang, Z.T., Li, B., Fang, C.M., Zhao, B., 2011. Assessing impact of land uses on land salinization in the Yellow River Delta, China using an integrated and spatial statistical model. Land Use Policy 28, 857–866.
Zhong, Q., Wang, K., Lai, Q., Zhang, C., Zheng, L., Wang, J., 2016. Carbon dioxide fluxes and their environmental control in a reclaimed Coastal Wetland in the Yangtze Estuary. Estuar. Coast. 39, 344–362.